Available online at www.sciencedirect.com
ScienceDirect
Earth and Planetary Science Letters 252 (2006) 342–359
EPSL
www.elsevier.com/locate/epsl

Modes of planetary-scale Fe isotope fractionation

Ronny Schoenberg *, Friedhelm von Blanckenburg

Institute for Mineralogy, University of Hannover, Callinstrasse 3, D-30167 Hannover, Germany

Received 2 February 2006; received in revised form 29 September 2006; accepted 30 September 2006
Available online 9 November 2006
Editor: R.W. Carlson

Abstract

A comprehensive set of high-precision Fe isotope data for the principle meteorite types and silicate reservoirs of the Earth is used to investigate iron isotope fractionation at inter- and intra-planetary scales. 14 chondrite analyses yield a homogeneous Fe isotope composition with an average $\delta^{56}Fe/^{54}Fe$ value of -0.015 ± 0.020‰ (2 SE) relative to the international iron standard IRMM-014. Eight non-cumulate and polymict eucrite meteorites that sample the silicate portion of the HED (howardite–eucrite–diogenite) parent body yield an average $\delta^{56}Fe/^{54}Fe$ value of -0.001 ± 0.017‰, indistinguishable to the chondritic Fe isotope composition. Fe isotope ratios that are indistinguishable to the chondritic value have also been published for SNC meteorites. This inner-solar system homogeneity in Fe isotopes suggests that planetary accretion itself did not significantly fractionate iron. Nine mantle xenoliths yield a 2σ envelope of -0.13‰ to $+0.09$‰ in $\delta^{56}Fe/^{54}Fe$. Using this range as proxy for the bulk silicate Earth in a mass balance model places the Fe isotope composition of the outer liquid core that contains ca. 83% of Earth's total iron to within ±0.020‰ of the chondritic $\delta^{56}Fe/^{54}Fe$ value. These calculations allow to interprete magmatic iron meteorites ($\delta^{56}Fe/^{54}Fe=+0.047\pm0.016$‰; $N=8$) to be representative for the Earth's inner metallic core. Eight terrestrial basalt samples yield a homogeneous Fe isotope composition with an average $\delta^{56}Fe/^{54}Fe$ value of $+0.072\pm0.016$‰. The observation that terrestrial basalts appear to be slightly heavier than mantle xenoliths and that thus partial mantle melting preferentially transfers heavy iron into the melt [S. Weyer, A.D. Anbar, G.P. Brey, C. Munker, K. Mezger and A.B. Woodland, Iron isotope fractionation during planetary differentiation, Earth and Planetary Science Letters 240(2), 251–264, 2005.] is intriguing, but also raises some important questions: first it is questionable whether the Fe isotope composition of lithospheric mantle xenoliths are representative for an undisturbed melt source, and second, HED and SNC meteorites, representing melting products of 4Vesta and Mars silicate mantles would be expected to show a similar fractionation towards heavy isotope compositions. This is not observed. Four international granitoid standards with SiO_2 contents between 60 and 70 wt.% yield $\delta^{56}Fe/^{54}Fe$ values between 0.118‰ and 0.132‰. An investigation of the alpine Bergell igneous rock suite revealed a positive correlation between Fe isotope compositions and SiO_2 contents — from gabbros and tonalites ($\delta^{56}Fe/^{54}Fe\approx0.03$ to 0.09‰) to granodiorites and silicic dykes ($\delta^{56}Fe/^{54}Fe\approx0.14$ to 0.23‰). Although in this suite $\delta^{56}Fe/^{54}Fe$ correlates with $\delta^{18}O$ values and radiogenic isotopes, open-system behavior to explain the heavy iron is not undisputed. This is because an obvious assimilant with the required heavy Fe isotope composition has so far not been identified. Alternatively, the relatively heavy granite compositions might be obtained by fractional crystallisation of the melt. Ultimately, further detailed studies on natural rocks and the experimental determination of mineral/melt fractionation factors at magmatic conditions are required to unravel whether or not iron isotope fractionation takes place during partial mantle melting and crystal fractionation.

Keywords: iron isotopes; solar system; planetary differentiation; crystal fractionation; granite

* Corresponding author. Tel.: +49 511 762 5998; fax: +49 511 762 2110.
E-mail address: r.schoenberg@mineralogie.uni-hannover.de (R. Schoenberg).

0012-821X/$ - see front matter © 2006 Elsevier B.V. All rights reserved.
doi:10.1016/j.epsl.2006.09.045

1. Introduction

The stable isotopes of iron undergo mass-dependent isotope fractionation during chemical and physical transport processes at the surface and within the Earth (e.g. [2–9]). Stable iron isotopes have also become an important tool in cosmochemistry. The first discovery made with this new isotope system was the finding that the Fe isotope compositions of different types of chondrites and achondrites, chondrules, and terrestrial rocks and mineral phases [10–13] all fall onto a mass-dependent fractionation line when plotted in a three-isotope space (i.e. $^{57}Fe/^{54}Fe$ vs. $^{56}Fe/^{54}Fe$ or $^{58}Fe/^{54}Fe$ vs. $^{56}Fe/^{54}Fe$). Based on these findings it was suggested that all nucleosynthetic Fe isotope heterogeneities – except ^{58}Fe anomalies in some very rare FUN-inclusions [14] – were homogenised in the solar nebula before the onset of chondrule formation and planetary accretion [10]. Yet although the existence of a uniform Fe source for the solar nebula was established early on, resolvable mass-dependent Fe isotope variations were found for different planetary materials. For example substantial variations exist between chondrules of chondrites [10,11,15]. Differences in the Fe isotope composition of approximately 0.07 to 0.15‰ in $^{56}Fe/^{54}Fe$ ratios were found for Earth and Moon when compared to Mars and 4Vesta [1,16]. The observed heavy Fe isotope composition of Earth and Moon was explained either by kinetic isotope fractionation through partial vaporisation during accretion and the giant Moon-forming impact event [16], or by melting and differentiation processes [1]. Bulk iron meteorites too were found to be relatively uniform in Fe isotope composition [10,17], despite significant inter-mineral variations [17]. Olivines in pallasites have been shown to contain very similar Fe isotope compositions, but published Fe isotope data for pallasite metal appear to be controversial. Zhu et al. [18] and Poitrasson et al. [17] found pallasite metal to be consistently heavier than the corresponding olivine. Zhu et al. [18] suggested equilibrium Fe isotope fractionation during metal/silicate differentiation of the pallasite parent bodies to account for these differences. Poitrasson et al. [17] found equilibrium Fe isotope fractionation at approximately 1000 °C between the two phases to be consistent for some of their pallasite data, but not for others. These authors therefore proposed that the metal-silicate Fe isotope fractionation of pallasites at moderate temperatures and pressures cannot be transposed to the planetary scale. Weyer et al. [1], on the other hand, found that pallasite metals were heavier as well as lighter in Fe isotope composition than corresponding olivine that they interpreted as the result of late-stage differentiation and low-temperature phase exsolution processes. To date it is still debatable whether or not iron meteorites or pallasites carry any information about Fe isotope fractionation during planetary core formation.

Small but significant variations in Fe isotope composition have recently been reported for different igneous reservoirs on Earth [1,19,20] that were partly interpreted as the result of magmatic fractionation processes [1,20]. These new findings appear to contradict earlier notions for a homogeneous terrestrial baseline for Fe isotopes [12] or a mean mafic Earth Fe isotope composition [16]. However, the extent to which the Fe isotope composition of terrestrial silicate reservoirs could be affected by such magmatic processes on the global scale remains yet to be investigated. So far a full understanding of the processes that may fractionate Fe isotopes in igneous systems has not even closely been established.

In order to provide a comprehensive description of Fe isotope compositions for different planetary bodies and different terrestrial reservoirs we examined (i) the Fe isotope systematics of our solar system, and (ii) the likelihood of intra-planetary Fe isotope fractionation during planetary differentiation and magma evolution processes. To this end, we determined by high-precision MC-ICP-MS the Fe isotope composition of different groups of chondrites, eucrites, and iron meteorites, as well as that of different terrestrial igneous reservoirs such as mantle xenoliths, ultramafic cumulates, basalts, and granites. In addition, to investigate possible Fe isotope fractionation during magma evolution at crustal levels, we determined the Fe isotope composition of igneous rocks from the well-characterised calc-alkaline Bergell intrusion, Central Alps [21].

2. Analytical methods

Samples were prepared for isotope analyses according to the procedure of Schoenberg and von Blanckenburg [22]. Iron isotope data are reported in the δ notation as the per mil deviation of the $^{56}Fe/^{54}Fe$, $^{57}Fe/^{54}Fe$, and $^{58}Fe/^{54}Fe$ ratios of a sample from the respective ratios of the international Fe metal standard IRMM-014 [23]:

$$\delta^{56}Fe_{Sample} = \left(\frac{{}^{56}Fe/{}^{54}Fe_{Sample}}{{}^{56}Fe/{}^{54}Fe_{IRMM-014}} - 1 \right) \times 1000 \quad [‰]$$

All Fe isotope measurements were performed on a ThermoFinnigan Neptune multi-collector inductively coupled plasma mass spectrometer in medium- and high-mass resolution modes [24]. Standard-sample

bracketing (SSB) and for most samples also Cu-doping (see [22,25]) were used to correct for the instrumental mass bias. Accuracy and precision of both mass bias correction methods were found to be identical [22]. All Fe isotope data used in this study refer to SSB corrected values. Fe isotope work in planetary reservoirs aims at resolving isotope ratio differences that are at the limit of the achievable analytical resolution. A comprehensive description of tests that were performed to exclude even minute (<0.05‰) artefacts introduced by sample processing and mass spectrometry is given as supplementary data in the electronic Appendix. No mass-independent effects were observed on any of the samples. Therefore we discuss our results in terms of δ^{56}Fe values only. Overall sample reproducibility of different laboratories for terrestrial and extraterrestrial samples is excellent (see Table A1 in the electronic Appendix) and thus allows direct comparison of published data with our own.

3. Results

3.1. Meteorite samples

3.1.1. Chondrites

δ^{56}Fe values from five carbonaceous, five ordinary and four enstatite chondrites vary between −0.068 and +0.036‰ (Table 1) and are in good agreement with published chondrite Fe isotope values [10,11,16,17,26] (Fig. 1). Two-tailed heteroscedastic student *t*-tests (i.e. assuming unequal variances) reveal that the three chondrite types cannot be distinguished from each other in their Fe isotope compositions (Table 2). Combining the Fe isotope measurements of all 14 chondrites yields an error-weighted mean δ^{56}Fe of −0.015±0.020‰ (uncertainty given at the 95% confidence level calculated by Isoplot [27] as $t \times \sigma \times \sqrt{\text{MSWD}}$ with t referring to the student *t*-factor for the degree of freedom of the population; uncertainties of our data of this kind are from hereon referred to as 2 SE). Different compounds of chondrites – metal, CAIs, and especially chondrules – are extremely heterogeneous in their Fe isotope compositions [10,11,15] and therefore appropriately sized aliquots of 10 to 20 mg from well-homogenised sample powders of 1 to 3 g were digested to avoid nugget effects. The light Fe isotope composition of the CB chondrite Bencubbin (chondrule-free matrix) is in agreement with previous measurements of CB metal and bulk samples [28]. Zipfel and Weyer [28] suggested that CB chondrites most likely condensated from a vapour cloud that was produced by a giant impact and that was thus depleted in heavy iron isotopes.

3.1.2. Eucrites

Aliquots of 10 to 20 mg from well-homogenised ca. 1 g eucrite powders were digested for Fe isotope analyses. The Fe isotope compositions of eight non-cumulate and polymict eucrites (supposed to originate from the asteroid 4Vesta) are very consistent and only vary from −0.016 to +0.021‰ in δ^{56}Fe (Table 1; Fig. 1). The error-weighted mean δ^{56}Fe of −0.001±0.017‰ (2 SE) of our eucrite measurements agrees well with Poitrasson et al.'s [16] average eucrite and diogenite δ^{56}Fe value of +0.020±0.016‰ (N=9), that was recalculated from their measured δ^{57}Fe/^{54}Fe value, and Weyer et al.'s [1] δ^{56}Fe value of +0.019±0.019‰ (N=4). Student *t*-tests reveal that the eucrite Fe isotope composition cannot be distinguished from that of the chondrites (Table 2). The Fe isotope composition of eucrites is also indistinguishable to those of SNC-meteorites [1,16] that are supposed to represent Mars. Due to the overall agreement between published data [1,16] and those reported here, the Fe isotope compositions of SNC-meteorites also appear to be indistinguishable to those of chondrites.

3.1.3. Iron meteorites

Between ca. 30 and 50 mg of drill chips from the different iron meteorites were digested for Fe isotope analyses. The Fe isotope compositions of magmatic iron meteorites only vary between 0.015 and 0.078‰ in δ^{56}Fe, in agreement with published data [10,11,17] (Table 1; Fig. 1). The error-weighted mean δ^{56}Fe value of the magmatic iron meteorite data reported here is 0.047±0.016‰. Student *t*-tests show that the Fe isotope composition of magmatic iron meteorites is clearly distinct to those of chondrites (see also [17]) at the 99.9% confidence level (Table 2). The Fe isotope compositions of our and published [10,11,17] non-magmatic IAB-IIICD iron meteorites seem to vary stronger than those of the magmatic groups (Table 1; Fig. 1), with our samples covering a range of −0.069 to 0.103‰ in δ^{56}Fe and published δ^{56}Fe values of up to 0.191‰ [1].

Taenite and kamacite, the two most prominent mineral phases of iron meteorites, appear to have slightly dissimilar Fe isotope compositions with taenite being isotopically heavier than kamacite [17]. Taenite and kamacite Fe isotope compositions of the two non-magmatic iron meteorites Toluca (IAB) and Cranbourne (IIICD) determined by Poitrasson et al. [17] ranged from 0.044 to 0.239‰ in δ^{56}Fe. However, the δ^{56}Fe value of our bulk Toluca sample of −0.069‰ – although being confirmed by femtosecond laser ablation MC-ICP-MS measurements of kamacite on the same sample yielding δ^{56}Fe=−0.06±0.06‰ [29] – is lower than those of Toluca taenite and kamacite reported by Poitrasson et al.

Table 1
Fe isotope composition of chondrites, eucrites and iron meteorites

Sample	$run#	SSB corrected			Cu-doping corrected		
		δ^{56}Fe±*2σ	δ^{57}Fe±*2σ	δ^{58}Fe±*2σ	δ^{56}Fe±*2σ	δ^{57}Fe±*2σ	δ^{58}Fe±*2σ
Carbonaceous chondrites							
Allende BE-412-2 CV3	3	−0.015±90	−0.005±183	−0.09±41	−0.048±42	−0.025±71	−0.28±52
Allende Brisbane CV3	2	−0.012±46	−0.001±73	−0.01±41			
Axtell CV3	3	0.003±59	0.024±73	−0.01±41			
SAU "CV3" (unnamed chondrite)	1	−0.053±46	−0.092±73	−0.30±41	−0.052±42	−0.091±71	−0.30±52
Murchison BE-460 CM2	2	−0.062±46	−0.082±73	−0.08±41			
Bencubbin-matrix CB	2	−0.171±46	−0.232±73	−0.33±41			
Ordinary chondrites							
Dar al Gani 300 H3–H5	2	−0.023±46	−0.028±73	−0.06±57			
Homestead L5	2	0.036±46	0.058±73	0.03±41			
Mt. Tazerait L5	2	−0.034±46	−0.016±73	−0.08±41			
Dar al Gani 298 LL4	2	0.025±46	0.072±73	0.20±41			
Djoumine H5–H6	2	−0.068±46	−0.065±73	−0.25±41			
Enstatite chondrites							
Sahara EH3	4	−0.005±46	−0.007±73	0.00±41			
Abee EH4	3	0.032±55	0.062±73	0.07±41			
Atlanta EL6	4	−0.020±77	−0.030±155	−0.14±41			
Eagle EL6	4	0.014±57	0.019±84	0.01±41			
£*Mean chondrites*		*−0.015±20*	*−0.006±32*	*−0.05±11*			
Eucrites							
Cachari (non-cumulate)	2	−0.004±58	0.008±73	−0.02±41			
Camel Donga (non-cumulate)	2	−0.001±50	−0.016±79	0.03±41			
Jonzac (non-cumulate)	2	−0.016±62	−0.002±117	−0.05±41			
Juvinas non-cumulate)	2	−0.008±46	−0.007±73	−0.02±41			
Stannern (non-cumulate)	2	−0.003±46	−0.017±73	−0.05±41			
Millbillillie (polymict)	2	0.021±46	0.024±73	−0.05±41			
Padvarninkai (polymict)	2	0.010±46	0.006±73	0.04±41			
Pasamonte (polymict)	2	−0.013±46	0.007±73	0.02±41			
Mean eucrites		*−0.001±17*	*0.001±27*	*−0.01±14*			
Iron meteorites							
Arispe IC (magmatic)	1	0.078±46	0.171±73	0.14±41	0.090±42	0.188±71	0.16±52
Locust Grove IIAB (magmatic)	1	0.031±46	0.058±73	0.17±41	0.043±42	0.076±71	0.19±52
North Chile IIAB (magmatic)	1	0.030±46	0.127±73	0.04±41	0.071±42	0.188±71	0.12±52
Cape York IIIAB (magmatic)	1	0.049±46	0.093±73	0.63±41	0.036±42	0.073±71	0.60±52
Ruffs Mountain IIIAB (magmatic)	1	0.015±46	0.024±73	0.01±41	0.023±42	0.036±71	0.03±52
Hvizo Pa IVA (magmatic)	1	0.032±46	0.013±73	−0.08±41	0.015±42	−0.013±71	−0.11±52
Hoba IVB (magmatic)	1	0.072±46	0.093±73	−0.10±41			
Santa Clara IVB (magmatic)	2	0.072±46	0.123±73	0.26±41	0.074±42	0.126±71	0.27±52
Mean magmatic iron meteorites		*0.047±16*	*0.088±45*	*0.13±20*	*0.050±26*	*0.096±70*	*0.18±19*
Canon Diablo IAB (non-magm.)		10.103±46	0.148±73	−0.18±41			
Odessa IAB (non-magm.)	1	0.060±46	0.053±73	0.19±41	0.045±42	0.032±71	0.16±52
Toluca IAB (non-magm.)	1	−0.069±46	−0.023±73	−0.48±41	−0.100±42	−0.070±71	−0.54±52
Nantan IIICD (non-magm.)	1	0.068±46	0.146±73	0.11±41	0.067±42	0.144±71	0.10±52
Mean non-magmatic iron meteorites		*0.04±12*	*0.08±13*	*−0.09±48*	*0.00±23*	*0.04±27*	*−0.09±96*
Glenormiston (ungrouped)	1	0.025±46	0.045±73	−0.09±41	0.021±42	0.039±71	−0.10±52
Pinon (ungrouped)	1	0.028±46	0.107±73	0.26±41	0.020±42	0.094±71	0.24±52

*Given as the 2 standard deviation reproducibility of replicate measurements, internal measuring precision for single analysis, or external reproducibility of our JM Fe standard [22], whichever was largest. Numbers refer to the last digits given for the respective δ-values.
$Refers to SSB corrected data only. No replicate measurements were performed with the Cu-doping correction method.
£Bencubbin-matrix omitted for calculation.

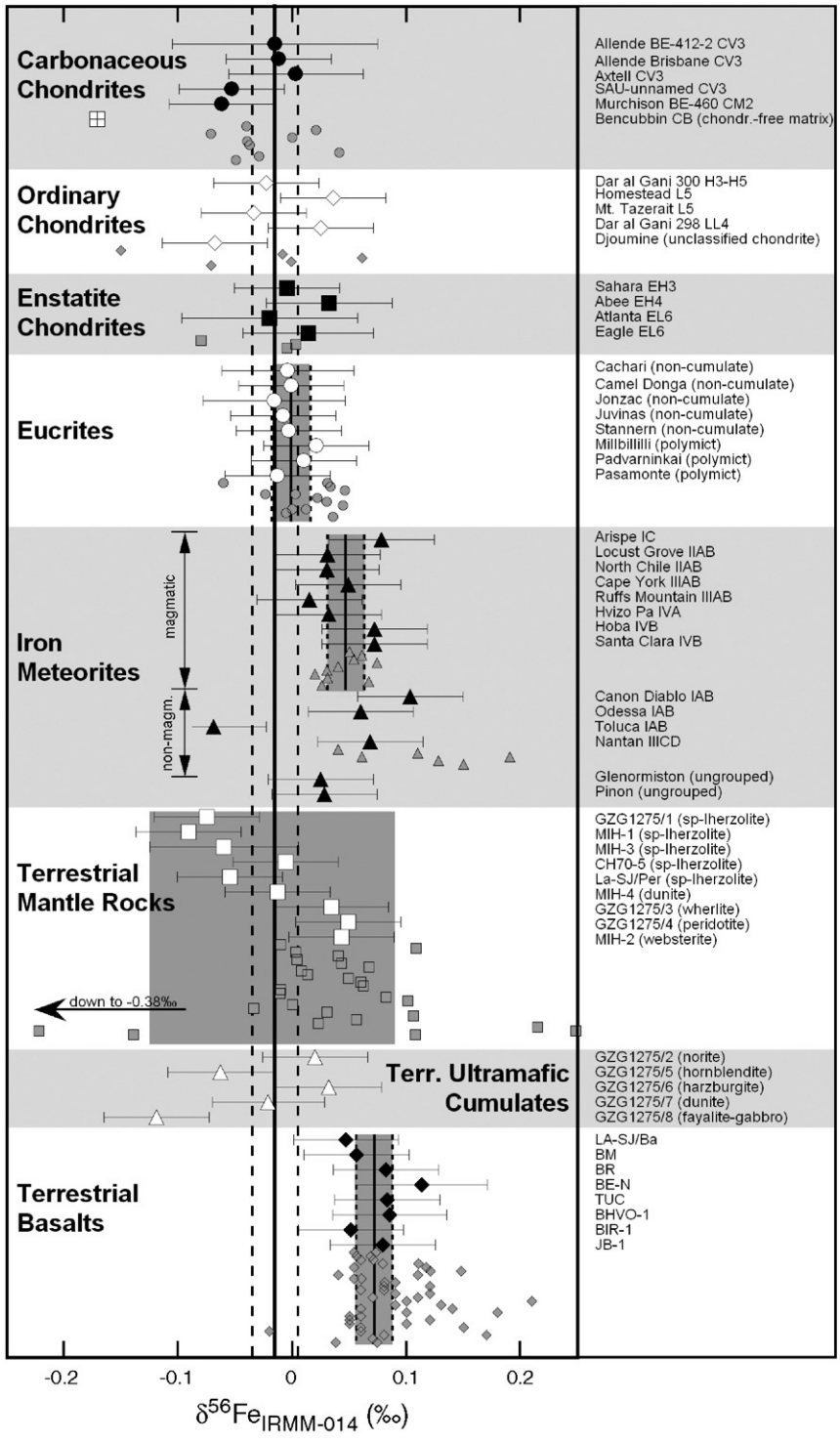

Fig. 1. δ^{56}Fe values of different meteorite groups and terrestrial rock reservoirs. The coarse solid and stippled lines give the weighted mean and 2 standard error uncertainty limits of the δ^{56}Fe of combined chondrite samples (Table 1). The fine solid and stippled lines (areas underlain in grey) give the weighted mean and 2 standard error uncertainty limits of the respective sample groups. Grey symbols represent published data of the respective sample groups ([1,10,11,16,19,20,26]).

Table 2
Student *t*-test results for comparison of different meteorite populations and terrestrial basalts

Population 1	Population 2	*t*-calculated	*df**	*t*-critical at a probability of		
				$p=0.05$	$p=0.01$	$p=0.001$
Carbonaceous chondrites	Ordinary chondrites	0.65	8	2.31	3.36	5.04
Carbonaceous chondrites	Enstatite chondrites	1.94	7	2.37	3.50	5.41
Ordinary chondrites	Enstatite chondrites	0.79	7	2.37	3.50	5.41
Chondrites (all groups)	Eucrites	1.14	20	2.09	2.85	3.85
Chondrites (all groups)	Iron meteorites	4.91	20	2.09	2.85	3.85
Chondrites (all groups)	Terrestrial basalts	7.37	20	2.09	2.85	3.85

*Degree of freedom.

[17]. A possible explanation for this discrepancy may be sample heterogeneity, most likely as a result of strongly varying kamacite/taenite ratios between relatively small specimens from the same meteorite. Such within-sample variability of metal Fe isotope composition has been reported for pallasite metals [1,10,17] and might also be likely for iron meteorite metals. There is no obvious reason why non-magmatic iron meteorites should be more affected by sample heterogeneity than magmatic ones. However, given the small number of bulk sample and mineral Fe isotope data of iron meteorites, the heterogeneity in δ^{56}Fe values on the mineral scale and the problem of sample homogeneity due to large crystal sizes as has been mentioned earlier [17], a more detailed investigation of the Fe isotope systematics of the various groups of this meteorite class is needed.

3.2. Terrestrial samples

Approximately 50 to 100 g of all terrestrial rocks were thoroughly powdered in agate mills. From these well-homogenised powder sample aliquots of 50 to 100 mg were digested for Fe isotope analyses.

3.2.1. Mantle xenoliths and ultramafic cumulates

X-ray fluorescence major element data for all mantle xenoliths and ultramafic cumulates except for the websterite sample MIH-Per/2 are given in Table 3. δ^{56}Fe values of mantle xenoliths and ultramafic cumulates reported here range from −0.091 to +0.049‰ and −0.119 to +0.032‰ (Table 4; Fig. 1), respectively. This is a much larger spread than that reported for chondrites and achondrites. Large variations in δ^{56}Fe values for mantle xenoliths and their mineral phases have already been reported [19,30,31]. Especially spinel–peridotites tend to contain light Fe with δ^{56}Fe values as negative as −0.38‰ [19], while garnet–lherzolites tend towards heavy Fe isotope compositions of up to +0.25‰ in δ^{56}Fe [19,30] (Fig. 1).

3.2.2. Basalts

The Fe isotope compositions of eight terrestrial oceanic and continental basalts given in Table 4 cover a very narrow range with an error weighted average δ^{56}Fe value of +0.072±0.016‰ (2 SE). This value agrees well with published Fe isotope data of basalts by Beard et al. ([12]; δ^{56}Fe=+0.094±0.016‰ (2 SE), $N=31$), Poitrasson et al. ([16]; δ^{56}Fe=+0.072±0.029‰ (2 SE) recalculated from their δ^{57}Fe data, $N=4$), and Weyer et al. ([32]; δ^{56}Fe=+0.076±0.029‰ (2 SE), $N=6$). Student *t*-tests (Table 2) reveal that the Fe isotope composition of terrestrial basalts can be clearly distinguished from that of chondrites at a confidence level of 99.9%.

3.2.3. Granitoids and Bergell igneous rocks

The four international granitoid standards GA, GS-N, SDC-1, and STM-1 (with SiO_2 between 60 and 70 wt.%) yield δ^{56}Fe values between +0.118‰ and +0.132‰ (Table 4; Fig. 2). The Fe isotope compositions of additional international and in-house rock standards, most of which are mafic in composition, but neither of clear peridotitic, basaltic, or granitoid origin (listed as "Others" in Table 4) lie between 0.017 and 0.065‰ in δ^{56}Fe; the peralkaline rhyolite NSL (SiO_2 = 75.45 wt.%) has a δ^{56}Fe value of 0.302‰ which is the heaviest Fe isotope composition reported in this study.

The rocks from the Bergell igneous intrusion reveal a slight trend towards heavier Fe isotope compositions from gabbros/tonalites over granodiorites to aplite/pegmatite dykes (Table 4). The Fe isotope compositions of hornblende–pyroxene–olivine–cumulates are amongst the lightest found for Bergell rocks. Note that for the Bergell rocks uncertainties in Table 4 were given as external reproducibilities or 2 standard deviations of the population, while in Figs. 2, 4, and 5) we applied the external reproducibility of pooled measurements of ±0.021‰ to the average δ^{56}Fe values (see Fig. A2 of the electronic Appendix). Similar reproducibilities of

Table 3
Major element compositions of mantle xenoliths and ultramafic cumulates

	GZG 1275/1	GZG 1275/2	GZG 1275/3	GZG 1275/4	GZG 1275/5	GZG 1276/6	GZG 1275/7	GZG 1275/8	MIH-Per/1	MIH-Per/3	MIH-Per/4	CH70-5	LA-SJ/Per
	Sp-lherzolite	Norite	Wherlite	Peridotite	Hornblendite	Harzburgite	Dunite	Fayalite-gabbro	Sp-lherzolite	Sp-lherzolite	Dunite	Sp-lherzolite	Sp-lherzolite
	Ivrea-Verbano Zone	Hitterø	Frankenstein/ Odenwald	Radauthal/ Harz mountains	Schriesheim/ Baden	Burgersford/ Bushveld Complex	Driekop Mine/ Bushveld complex	Bad Harzburg/ Harz mountains	Finero/ Ivrea-Verbano zone	Meerfelder Maar/Eifel	Locality unknown	Val Moleno	Salinas de Janubio/ Lanzarote
	Italy	Norway	Germany	Germany	Germany	South Africa	South Africa	Germany	Italy	Germany	New Zealand	Switzerland	Canary Isl.
	wt.% of oxide components												
SiO_2	43.39	50.55	36.91	38.76	44.64	47.16	37.22	36.27	44.34	43.49	39.93	43.69	44.37
TiO_2	0.45	1.45	0.24	0.15	0.48	0.18	0.02	2.66	0.01	0.02	0.01	0.04	0.06
Al_2O_3	7.22	22.62	3.53	6.99	5.68	6.22	0.11	20.48	0.88	0.89	0.45	1.22	1.51
Fe_2O_{3total}	8.50	7.07	15.69	10.19	10.80	9.11	17.94	19.30	8.72	9.23	8.72	9.36	8.44
MnO	0.13	0.07	0.24	0.14	0.18	0.14	0.24	0.13	0.12	0.11	0.12	0.13	0.13
MgO	33.08	4.46	29.23	29.21	22.99	28.78	40.30	15.00	44.00	45.11	48.15	43.25	43.29
CaO	5.88	8.56	2.76	3.85	8.64	3.72	0.24	1.02	0.97	0.57	0.24	0.07	1.03
Na_2O	0.20	3.85	<0.01	0.04	0.65	0.54	<0.01	0.31	<0.01	<0.01	<0.01	<0.01	<0.01
K_2O	0.02	0.66	0.14	0.18	0.54	0.36	0.01	3.37	0.02	0.01	0.01	0.02	0.08
P_2O_5	0.01	0.06	0.02	0.02	0.12	0.04	0.00	0.53	<0.001	0.00	0.00	0.00	0.02
Total	99.17	99.66	99.43	99.20	99.51	99.09	99.27	99.55	99.15	99.27	98.61	99.15	98.64

Table 4
Fe isotope composition of terrestrial igneous rocks

Sample	$run#	SSB corrected			Cu-doping corrected		
		δ^{56}Fe±*2σ	δ^{57}Fe±*2σ	δ^{58}Fe±*2σ	δ^{56}Fe±*2σ	δ^{57}Fe±*2σ	δ^{58}Fe±*2σ
Mantle rocks							
GZG1275/1 (sp-lherzolite)	1	−0.075±46	−0.083±73	0.17±41	−0.086±42	−0.100±71	0.15±52
GZG1275/3 (wherlite)	1	0.034±50	0.046±73	−0.25±41			
GZG1275/4 (peridotite)	2§	0.049±46	0.069±73	−0.27±41	0.108±42	0.138±71	−0.53±52
MIH-Per/1 (sp-lherzolite)	1	−0.091±46	−0.162±73	0.22±41	−0.097±42	−0.171±71	0.21±52
MIH-Per/2 (websterite)	1	0.043±46	0.024±73	0.41±41	0.028±42	0.002±71	0.38±52
MIH-Per/3 (sp-lherzolite)	2§	−0.060±65	−0.091±73	−0.49±41	−0.045±42	−0.088±71	−0.83±52
MIH-Per/4 (dunite)	2§	−0.013±46	−0.021±73	−0.14±41	−0.019±42	−0.007±71	−0.28±52
CH70-5 (sp-lherzolite)	1	−0.006±46	0.012±73	0.45±41			
LA-SJ/Per (sp-lherzolite)	1	−0.055±46	−0.055±73	−0.19±41	−0.050±42	− 0.048±71	−0.18±52
Mean peridotites		*−0.018±41*	*−0.029±58*	*−0.01±25*	*−0.014±34*	*−0.039±91*	*−0.15±40*
Ultramafic cumulates							
GZG1275/2 (norite)	2§	0.020±46	0.036±73	−0.18±41	0.031±42	0.056±71	−0.54±52
GZG1275/5 (hornblendite) (Nr.52)	2§	−0.063±46	−0.065±73	−0.42±41	−0.049±42	−0.030±71	−0.58±52
GZG1275/6 (harzburgite)	2§	0.032±46	0.055±99	−0.23±41	0.030±42	0.070±71	−0.32±52
GZG1275/7 (dunite)	1	−0.021±49	−0.072±73	−0.21±41			
GZG1275/8 (fayalite-gabbro)	1	−0.119±46	−0.200±73	0.01±41			
Continental and oceanic basalts							
LA-SJ/Ba (in-house basalt)	1	0.047±46	0.088±73	−0.14±41	0.076±42	0.130±71	−0.09±52
BM (ZGI basalt)	1	0.056±46	0.109±73	0.01±41	−0.013±42	0.007±71	−0.13±52
BR (CRPG basalt)	1	0.082±46	0.073±73	0.26±41	0.080±42	0.069±71	0.25±52
BE-N (CRPG basalt)	3§	0.113±58	0.187±86	0.33±42	0.091±42	0.156±71	0.28±52
TUC (in-house basalt)	1	0.083±46	0.155±73	−0.05±41	0.126±42	0.221±71	0.03±52
BHVO-1 (USGS basalt)	4§	0.085±50	0.111±86	0.14±57	0.063±42	0.074±71	0.51±52
BIR-1 (USGS basalt)	4§	0.051±46	0.063±73	0.07±41	0.002±42	−0.015±71	−0.56±52
JB-1 (GSJ basalt)	2	0.079±46	0.074±73	−0.13±41	0.069±42	0.029±71	−0.36±52
Mean basalts		*0.072±16*	*0.104±35*	*0.05±15*	*0.062±15*	*0.084±25*	*−0.01±18*
Granitoids∈							
GA (CRPG granite)	3§	0.120±85	0.185±124	0.14±41	0.140±42	0.218±71	0.43±52
GS-N (CRPG granite)	3§	0.129±46	0.177±73	0.30±45	0.134±42	0.182±71	0.24±52
STM-1 (USGS syenite)	2§	0.132±46	0.197±80	0.36±41			
NSL (in-house peralk. rhyolite)	2	0.302±46	0.439±73	0.783±41			
Others							
SDC-1 (USGS mica-schist)	2§	0.118±83	0.157±106	0.45±41	0.142±42	0.185±71	0.72±52
AN-G (CRPG anorthosite)	1	0.065±46	0.088±73	0.34±41	0.046±42	0.060±71	0.30±52
DNC-1 (USGS dolerite)	2	0.017±46	0.028±73	−0.12±41	0.012±42	0.014±71	−0.14±52
W-2 (USGS diabase)	2	0.036±93	0.026±89	0.20±41	0.022±42	−0.012±71	0.40±52
SDO-1 (USGS shale)	2	0.036±46	0.060±73	0.08±41	0.008±42	0.019±71	0.18±52
89092 (in-house Gabbro)	9	0.057±46	0.068±73	0.14±41			
Bergell intrusion, Central Alps							
Siss6 (Hbl-cumulate)	5	−0.005±46	−0.009±86	− 0.12±62	0.010±42	0.027±71	0.06±52
Siss4 (Hbl-cumulate)	5	0.040±46	0.051±74	−0.06±59	0.046±42	0.029±71	−0.29±52
Siss1 (gabbro)	5	0.053±51	0.066±103	0.01±41	0.066±42	0.103±71	−0.18±52
Siss2 (gabbro)	5	0.028±51	0.032±100	0.18±41	0.060±42	0.041±71	0.29±52
Siss5b (gabbro)	5	0.048±65	0.047±73	0.17±41	0.083±42	0.054±71	0.37±52
Siss5a (gabbro)	5	0.088±46	0.122±73	0.29±41	0.070±42	0.083±71	0.31±52
Malf1 (basalt)	5	0.064±46	0.087±73	0.12±41			
Iorio2 (tonalite)	5	0.055±46	0.065±73	0.05±81	0.066±42	0.075±71	−0.36±52
Sor1 (tonalite)	5	0.065±75	0.092±89	0.09±41	0.079±42	0.071±71	−0.01±52
Mer1 (tonalite)	5	0.061±46	0.078±89	0.06±41	0.081±42	0.141±71	0.15±52
Ma1 (tonalite)	5	0.062±52	0.068±82	0.31±47	0.060±42	0.073±71	0.24±52

(continued on next page)

Table 4 (*continued*)

Sample	$run#	SSB corrected			Cu-doping corrected		
		δ^{56}Fe±*2σ	δ^{57}Fe±*2σ	δ^{58}Fe±*2σ	δ^{56}Fe±*2σ	δ^{57}Fe±*2σ	δ^{58}Fe±*2σ
Bergell intrusion, Central Alps							
Ge20 (tonalite)	5	0.071±46	0.093±73	0.27±41	0.056±42	0.110±71	0.17±52
Iorio1 (augengneiss)	5	0.111±46	0.149±73	0.25±41	0.127±42	0.182±71	0.20±52
Bona1 (granodiorite)	5	0.097±46	0.161±73	0.26±41	0.112±42	0.153±71	0.4±52
Bona3 (roof pendant)	5	0.084±46	0.107±73	0.34±85	0.069±42	0.059±71	0.98±52
Loa1 (aplite)	5	0.147±46	0.206±73	0.25±52	0.163±42	0.229±71	0.56±52
Bona2 (aplite)	5	0.141±52	0.216±73	0.29±47	0.183±42	0.262±71	0.01±52
Siss7 (pegmatite)	5	0.226±46	0.334±73	0.45±41	0.251±42	0.318±71	0.48±52

*Given as the 2 standard deviation reproducibility of replicate measurements, internal measuring precision for single analysis, or external reproducibility of our JM Fe standard [22], whichever was largest. Numbers refer to the last digits given for the respective δ-values.
$Refers to SSB corrected data only. No replicate measurements were performed with the Cu-doping correction method.
§Data from at least two independent sample digestions.
ZGI=Zentrales Geologisches Institut, Berlin, former GDR; CRPG=Centre de Recherches Pétrographiques et Géochimiques, Vandoeuvre lès-Nancy, France; USGS=United States Geological Survey, Denver, USA; GSJ=Geological Survey of Japan.

pooled Fe isotope data were previously described for Fe isotope measurements with the ThermoFinnigan Neptune instrument [20].

4. Discussion

4.1. The Fe isotope composition of the inner solar system

Despite the large variations in δ^{56}Fe values of chondrules ranging from ~ −1.85 to 0.63‰ [10,11,15], bulk chondrite Fe isotope compositions are homogeneous with a weighted mean δ^{56}Fe of −0.015±0.020‰. The large Fe isotope variations of chondrules were interpreted as the result of partial Fe evaporation during chondrule formation [33,34] or aqueous alteration on the chondrite parent bodies [11]. Regardless of the actual cause of these large intra-chondrite variations it can be argued that Fe isotopes were homogenised in the solar nebula before the onset of chondrule formation and planetesimal accretion, because all these materials plot on a single mass-dependent fractionation line in three-isotope space [10] and Fe isotope variability between different meteorite types and terrestrial planetary bodies are small [17]. The homogeneity of the Fe isotope compositions of carbonaceous, ordinary, and enstatite chondrites reported in this study further indicates that there was no apparent mass-dependent Fe isotope gradient throughout at least the inner regions of the solar disc from which these three chondrite classes accreted. This observation opens the possibility for the existence of a chondritic uniform reservoir (CHUR) for Fe isotopes with a δ^{56}Fe value of −0.015±0.020‰ relative to IRMM-014 for the inner solar region from which the terrestrial planets accreted. Support for a CHUR Fe isotope composition for the bulk terrestrial planets is also given by the Fe isotope compositions of the silicate portions of Mars and 4Vesta that are indistinguishable to the chondritic composition ([1,16,17] and this study). However, the heavier Fe isotope compositions observed for terrestrial and lunar basalts compared to the chondritic compositions of SNC meteorites and eucrites place severe problems for a CHUR Fe isotope composition of the terrestrial planets. These are discussed in detail in Section 4.3.

4.2. Fe isotope fractionation by planetary core formation

In the following section we estimate maximum Fe isotope fractionation between the bulk silicate Earth and the Earth's metal core that can be expected as a result of core/mantle differentiation. To do so, we first need to constrain the Fe isotope composition of the bulk silicate Earth. From simple mass-balance considerations and possible high-temperature Fe isotope fractionation factors, potential Fe isotope compositions for the terrestrial core can then be inferred and compared to likely proxies such as iron meteorites. The aim here is to investigate the extent at which the terrestrial core formation can shift the Fe isotope compositions of the bulk silicate Earth and the metal core from that of the bulk Earth.

4.2.1. The Fe isotope composition of the bulk silicate Earth

The relatively large variation in δ^{56}Fe values of mantle xenoliths determined in this study ranging from −0.091‰ to +0.049‰ overlaps with the chondritic value and is within uncertainties indistinguishable to the mean mafic Earth Fe isotope composition with δ^{56}Fe=+0.068±0.020‰ (2 SE) suggested by Poitrasson et al. [16] and

close to the homogeneous terrestrial baseline for Fe isotopes with δ^{56}Fe=+0.090±0.015‰ (2 SE) proposed by Beard et al. [12]. Still larger variations for terrestrial mantle rocks ranging from −0.38‰ to +0.25‰ in δ^{56}Fe have already been published [19,31], although the bulk of published mantle xenolith data also have δ^{56}Fe values between ca. −0.03‰ and +0.11‰ (Fig. 1). In contrast to this Fe isotope heterogeneity of mantle xenoliths, Weyer et al. [1] reported a very homogeneous Fe isotope composition for seven bulk rock and four olivine separates of peridotite samples with a δ^{56}Fe value of +0.015±0.018‰.

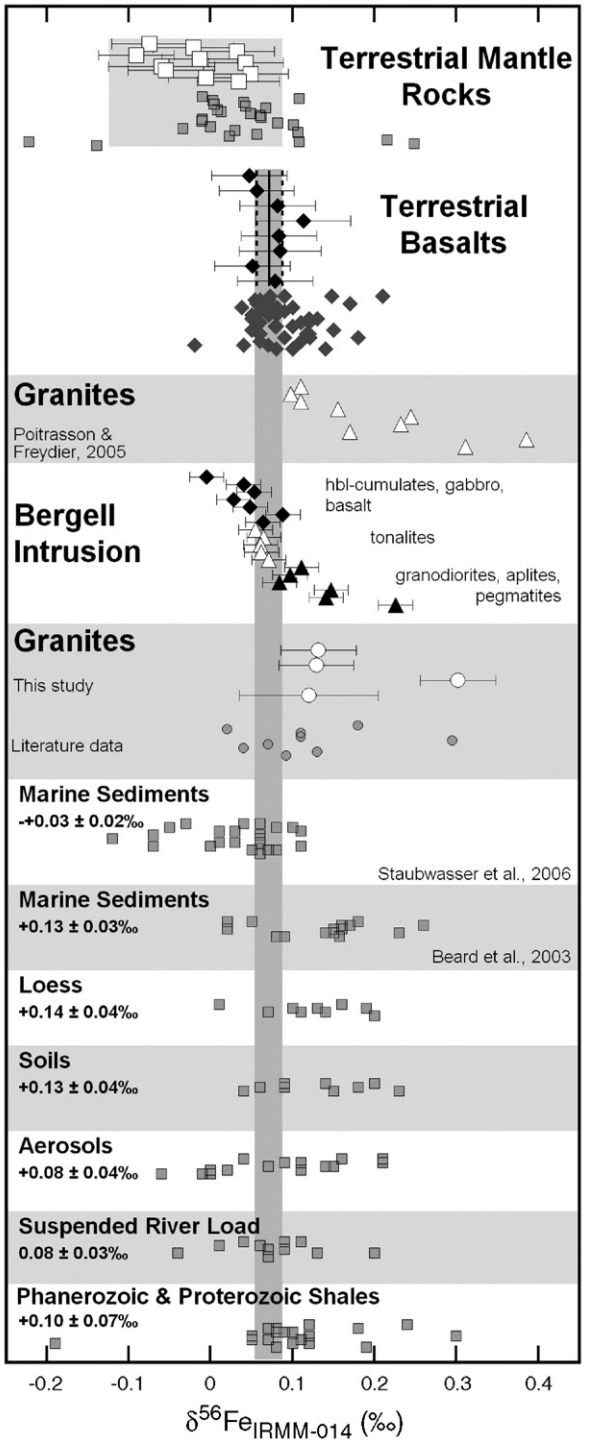

Notably, all mantle xenoliths investigated in the present study as well as in published works [1,19,31] originate from the lithospheric mantle. Thus, their Fe isotope compositions do not necessarily represent that of the silicate portion of our planet after core segregation (i.e. the bulk silicate Earth). Most likely some peridotite samples have undergone mantle metasomatism [30] and changes in mantle oxygen fugacity during partial melting that affected their original Fe isotope composition [19]. The large spread in δ^{56}Fe values of mantle rocks reported in this and other studies and the limitation of access to undepleted (asthenospheric) mantle xenoliths prevent us to unequivocally conclude that the Fe isotope composition of the bulk silicate Earth is either represented by that of chondrites or that of a homogeneous igneous reservoir [12,16]. Therefore, we use the two standard deviation limits of the Fe isotope composition of our mantle xenolith data (δ^{56}Fe of −0.13‰ to +0.09‰) as proxies for the bulk silicate Earth in the mass balance calculations that will follow. This range in δ^{56}Fe values includes all possible proxies for the bulk silicate Earth: (1) the chondritic Fe isotope composition reported in this study (δ^{56}Fe=−0.015±0.020‰); (2) the Fe isotope composition as deduced from mantle peridotites (+0.015±0.018‰; [1]); (3) the homogeneous terrestrial baseline for Fe isotopes [12] and the mean mafic Earth value [16]; (4) the bulk of δ^{56}Fe values of mantle peridotites determined so far (Fig. 1).

4.2.2. Proxies for the Fe isotope composition of Earth's core

Pallasites are believed to represent the interfaces between core and mantle of small planetesimals, while magmatic iron meteorites are thought to represent their inner metal cores. Published Fe isotope data of olivine, metal, schreibersite ($(Fe,Ni)_3P$) and troilite (FeS) of pallasites show large variations, but as lined out in the

Fig. 2. δ^{56}Fe values of different terrestrial igneous and sedimentary reservoirs. For comparison to other reservoirs the 2 standard error uncertainty limits of the δ^{56}Fe of our basalts are shown as vertical grey bar. Data for loess, soils, aerosols, suspended river loads, and shales are from Beard et al. [13]. All other samples with grey symbols are published data from [1,9,12,16,19,26,31,53]. Diagenetic iron cycling draws the iron of the marine sediments of Staubwasser et al. [56] towards lighter δ^{56}Fe values. Although these samples originate from two short drill cores of the Arabian Sea they illustrate the potential of low-temperature Fe isotope overprints on sedimentary rocks.

Introduction to this study they appear to yield contradictory results with regard to inter-mineral fractionation [1,17,18]. Therefore, we do not use any of the published pallasite data to infer planetary core Fe isotope compositions.

Bulk magmatic iron meteorites are much more homogenous in their isotope composition. Because the iron meteorites measured to date originate from different classes (Table 1), this uniformity may be considered to be a general feature of planetesimal cores with different fractions of metal crystallisation. There is also no indication to suggest that low-temperature processes would have modified the iron meteorites' bulk Fe isotope compositions. Therefore, we treat the somewhat heavier Fe isotope composition of iron meteorites compared to that of chondrites (see also [17]) as a genuine feature of metal–silicate differentiation on the parent bodies of these inner core remnants.

4.2.3. The Fe isotope composition of the metallic core and the silicate mantle

Calculating the iron budgets of Earth's major reservoirs using published reservoir sizes and Fe concentrations [35–38] reveals that the metal core amasses ~ 87% and the silicate mantle ~ 13% of Earth's total iron. Compared to these two terrestrial reservoirs the iron content of Earth's silicate crust is insignificant (i.e. ~ 1‰ of Earth's total iron). A simple mass balance calculation can be used to assess the Fe isotope composition of Earth's mantle. In a first step this calculation is based on two assumptions. (1) The bulk Earth has chondritic Fe isotope composition (i.e. δ^{56}Fe = −0.015‰), and (2) the Fe isotope composition of the Earth's core is represented by that of magmatic iron meteorites (with δ^{56}Fe = 0.047‰). In this model the Earth's silicate mantle is required to contain iron with a δ^{56}Fe value of −0.425‰; an Fe isotope composition that is much more negative than that of the lightest terrestrial mantle xenolith reported in this study (i.e. δ^{56}Fe of −0.119‰) and also lighter than those determined by Williams et al. ([19]; δ^{56}Fe of −0.38‰) and Weyer et al. ([1]; δ^{56}Fe of −0.024‰). A δ^{56}Fe value of −0.425‰ is also much lighter than the Fe isotope composition of any group of differentiated silicate meteorites determined so far, except the CB chondrites (see Section 3.1.1.). In addition, the $\Delta^{56}Fe_{metal-silicate} = \delta^{56}Fe_{core} - \delta^{56}Fe_{mantle}$ of 0.472‰ appears to exceed any predicted high-temperature Fe isotope fractionation between iron metal and silicate melt [39]. Temperatures of 2000 °C and 3000 °C were estimated for the interface between metal and silicate, respectively, in a deep magma ocean scenario [40–42]. Using the reduced partition function given by Polyakov and Mineev [39], predicted $\Delta^{56}Fe_{metal-olivine}$ values are only 0.017‰ to 0.008‰ at these temperatures.

A much better assumption is that the δ^{56}Fe value of 0.047‰ for magmatic iron meteorites can be a valid proxy for the inner solid planetary cores, rather than the entire core. In that case additional Fe isotope fractionation must have taken place between the solid inner core and the metal core melt from which it crystallised. Indeed magmatic iron meteorites are commonly believed to have formed by fractional crystallisation from metal core melts of small planetesimals [43]. During ongoing fractional crystallisation incompatible sulphur and phosphorus became enriched in the molten outer core and liquid immiscibility between S-rich and P-rich melts and the molten metal are likely to occur (e.g. [44]). Based on seismological density determinations enrichment of S, amongst other light elements, has also been proposed for the Earth's outer core [45]. Wood and Halliday [46] modelled late segregation of sulphur-rich metal to Earth's core after the Moon-forming giant impact to accommodate the discrepancy between U–Pb and Hf–W core formation chronometry. Schuessler et al. ([47]) experimentally determined the Fe isotope fractionation between pyrrhotite (FeS) and peralkaline silicate melt at a pressure of 500 MPa and temperatures between 840 and 1000 °C to be $\Delta^{56}Fe_{(pyrrhotite-melt)} = -0.35 \pm 0.04$‰. This value agrees well with new theoretical fractionation factors between troilite (FeS) and Fe-bearing silicates calculated from Moessbauer data (see [47]). Notably, the temperatures in the outer terrestrial core are much higher than those at which the experiments were run and the composition of the silicate mantle is of course not a peralkaline one. Still, the formation of an immiscible S-rich metal component in planetary cores or S-enriched outer metal cores during metal/silicate differentiation might have influenced the Fe isotope composition of the silicate mantle. Fig. 3 illustrates mass balance models for equilibrium Fe isotope fractionation between all the reservoirs that were involved in the terrestrial core formation using the parameters given in Table 5. For example, assuming that the bulk Earth Fe isotope composition equals CHUR (i.e. δ^{56}Fe = −0.015‰), the inner core has a near chondritic δ^{56}Fe value (i.e. ca. ±0.07‰ in δ^{56}Fe), and the silicate mantle has an Fe isotope composition between −0.13‰ and +0.09‰ in δ^{56}Fe (2 SD envelope of the mantle peridotites), then mass balance dictates that the outer S-bearing core has a δ^{56}Fe value that is within ca. ±0.02‰ of the CHUR value (Fig. 3). As lined out in Section 4.1 we do not unambiguously know whether or not the bulk silicate Earth Fe isotope composition is represented by that of chondrites or that of igneous rocks. We also don't know

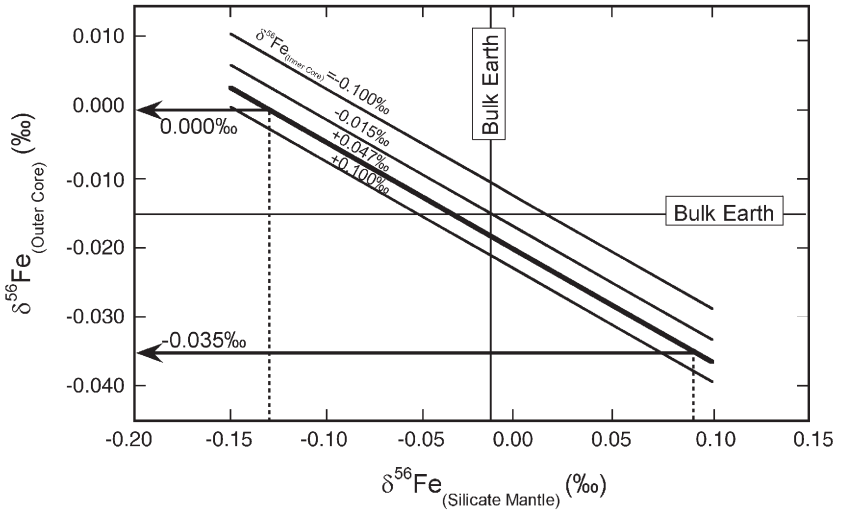

Fig. 3. Mass balance model for Earth's main reservoirs. Relevant parameters and δ^{56}Fe values of Earth's inner metallic core, the outer liquid core, and the silicate mantle used for the calculations are given in Table 5. Illustrated are Fe isotope compositions of the outer core required for silicate mantle δ^{56}Fe values as given on the *x*-axis. Possible inner metallic core Fe isotope compositions are contoured in the figure. The limits for δ^{56}Fe values of these inner core contour lines (i.e. +0.100 and −0.100‰) were chosen arbitrarily, and demonstrate the minute control of inner core compositions over outer core composition. The two fine dotted lines give the 2 standard deviation limits of mantle xenoliths and ultramafic terrestrial rocks determined in this study.

whether the bulk Earth has a chondritic iron isotope composition or is somewhat heavier due to partial evaporation and recondensation processes induced by the Moon-forming giant impact, as proposed by Poitrasson et al. [16]. However, if the Fe isotope composition of bulk Earth was significantly different to that of the CHUR, the outer core, containing most of the iron, would "buffer" the inner core and the silicate mantle to close isotope ratios, due to the small assumed fractionation factors at high temperatures. Therefore, a bulk Earth Fe isotope composition far from the CHUR value would be manifested by a bulk silicate Earth Fe isotope value far away from the chondritic one as well — a feature that is not observed for any terrestrial silicate rock reservoir.

Although the Fe isotope fractionation factors between metallic, sulfidic, and siliceous solids and melts at terrestrial core formation conditions are not yet known, the magnitude of the isotope ratio differences inferred here from mass balance are small (<0.1‰ in δ^{56}Fe), but in the range expected for these temperature conditions. It has to be mentioned that in the case of non-equilibrium Fe isotope fractionation between inner core, outer core, and silicate mantle bigger isotope effects may be expected, but again these are so far not observed for terrestrial silicate reservoirs.

4.3. Fe isotope fractionation during mantle melting

Weyer et al. [1] found that their average Fe isotope composition of mantle peridotites is significantly lower than that of terrestrial basalts. From this observation these authors concluded that partial mantle melting preferentially incorporates heavy iron into the melt. Indeed, the Fe isotope compositions of spinel–lherzolites reported in this study also appear to be lighter than the relatively homogeneous Fe isotope compositions of terrestrial basalts reported here and elsewhere [1,12,16] (Fig. 1). Preferential incorporation of heavy iron into the melt during mantle melting has also been discussed as potential explanation for the large variability of peridotite Fe isotope compositions [19].

Williams et al. [19] have presented a fractional melting model of mantle peridotite based on $\Delta^{56}Fe_{(mineral-melt)}$ of between −0.15 and −0.03‰. It was shown that melt fractions between 0 and 40% produce a very narrow range in δ^{56}Fe values for the resulting melts of only 0.02‰ with

Table 5
Model parameters to calculate the outer core Fe isotope composition by mass balance

Reservoir	Mass (kg)	Fe (wt.%)	total Fe (kg)	δ^{56}Fe (reservoir) (‰)
Bulk Earth	5.974×10^{24}	32.07	1.683×10^{24}	−0.015
Inner core	9.678×10^{22}	86.15	7.683×10^{22}	+0.100, +0.047[a], −0.015[b], −0.100
Outer core	1.835×10^{24}	86.15	1.457×10^{24}	Calculated
Silicate mantle	4.043×10^{24}	6.22	1.495×10^{23}	Variable between +0.09 and −0.13

[a]Average of magmatic iron meteorites determined in this study.
[b]Average of chondrites determined in this study.

the melt being ca. 0.07 – 0.13‰ heavier than the source, depending on the source mineral composition. Smaller melt Fe isotope variations for incongruent mantle melting were predicted if no mineral–melt fractionation occurred, in which case the melt had δ^{56}Fe values of ca. −0.02‰ to +0.02‰ relative to its source. However, Williams et al. [19] found that mantle melting alone fails to explain the large variability in Fe isotope compositions of mantle peridotites ([19,30,31]; to a lesser extent also in this study). Consequently, these authors suggested that, amongst other processes, changes in oxygen fugacity cause the Fe isotope variability observed for mantle rocks (see also [31]). Interestingly, whatever the source of terrestrial oceanic and continental basalts, be it fertile or depleted mantle, their Fe isotope compositions appear to be the same [12]. In any way, the strong variability of mantle peridotite Fe isotope composition itself limits the assignment of an unambiguous mantle Fe isotope signature.

In addition, the hypothesis of the incorporation of heavy iron isotopes into partial mantle melts relative to their source furthermore leads to a contradiction regarding SNC and eucrite/diogenite meteorites. These have significantly lighter Fe isotope compositions than terrestrial basalts. Rather, they are indistinguishable to the chondritic ratios ([1,16,20] and this study). Given that these meteorites represent partial mantle melts this is unexpected in light of the findings discussed above. It can be speculated that melt fractions were too high to produce significant fractionations, but there is no real indication to this from HED and SNC mineralogy and chemical composition. Alternatively, one could speculate that the modes of core formation and mantle oxygen fugacities were different from those of the Earth, thereby compensating for heavier melt compositions. A small difference in mantle oxidation state to that of the Earth has indeed been proposed for the HED parent body, but none was found for Mars [48]. Regardless of these caveats the possibility that heavy iron is enriched during partial mantle melting is an intriguing one, but further investigation of inter-mineral and mineral–melt fractionation in the mantle peridotite/basalt system are required to prove or disprove its existence.

4.4. Enrichment of evolved magmas in heavy Fe isotopes

Poitrasson and Freydier [20] determined heavy Fe isotope compositions for granites with $SiO_2 > 71$ wt.% and MgO < 0.6 wt.% (Fig. 2), in accord with our NSL peralkaline rhyolite (δ^{56}Fe = 0.302‰; SiO_2 = 75.45 wt.%, MgO below detection limit of ca. 0.01 wt.%) and the value for the granite standard AC-E (δ^{56}Fe = 0.295‰; SiO_2 = 70.35 wt.%, MgO = 0.03 wt.%) reported by Dauphas and Rouxel [49]. Poitrasson and Freydier [20] addressed these heavy Fe isotope signatures of granites to Fe isotope fractionation during late-stage fluid exsolution processes. From our own small dataset of granitic rocks (Fig. 2) it appears as if evolved granitoids with even lower SiO_2 contents may contain iron that is slightly heavier (δ^{56}Fe = 0.118–0.132‰) than the iron found in terrestrial basalts (δ^{56}Fe = 0.072 ± 0.016‰). Similarly, the Fe isotope compositions of different clastic sediments (but especially marine sediments, loess, and soils reported in [13]) that represent the upper continental crust also appear to be somewhat heavier than that of terrestrial basalts (Fig. 2), although not resolvable within the uncertainty limits of the average basalt value given in this study and the external reproducibility for Fe isotope measurements reported by Beard et al. [13]. However, heavy Fe isotope composition for evolved igneous rocks is in contrast to the findings of Beard and Johnson [30]. These authors did not measure any discernible differences in Fe isotope compositions for igneous rocks of any silica contents even for those with $SiO_2 > 71$ wt.% (see their Fig. 1).

In order to investigate possible Fe isotope fractionation during magma evolution we determined the Fe isotope composition of rocks from the calc-alkaline Bergell intrusion in the Swiss Alps. Bergell rocks analysed for Fe isotope compositions comprised basalts and gabbros (δ^{56}Fe = 0.03 to 0.06‰) and intermediate tonalites (δ^{56}Fe = 0.06 to 0.07‰) to granodiorites (δ^{56}Fe = 0.09 to 0.11‰). Aplites and pegmatites contain the heaviest Fe isotope composition with δ^{56}Fe of 0.14 to 0.23‰. Thus, δ^{56}Fe values of Bergell rocks positively correlate with SiO_2 contents (Fig. 4a), while negatively correlating with $Fe_2O_{3\ total}$ contents (Fig. 4b). Given these trends, one could argue that fractional crystallisation of a Fe-bearing phase removes light Fe isotopes, thus continuously enriching the residual melt in the magma chamber in heavy iron. However, radiogenic $^{87}Sr/^{86}Sr$ ratios and δ^{18}O values also increase with ongoing differentiation of the Bergell magma [21]. This is caused by the simultaneous assimilation of crustal material and fractional crystallisation (AFC), as is the case for most silica-saturated systems. Indeed, δ^{56}Fe values of the Bergell rocks positively correlate with δ^{18}O values (Fig. 4c). Therefore the increase towards heavy Fe isotope compositions of the Bergell granitoids with ongoing magma evolution might also be the result of open system behaviour meaning the continuous contamination with isotopically heavy host rock or lower crust, rather than one of fractional crystallisation. Both of these mechanisms are discussed in the following sections.

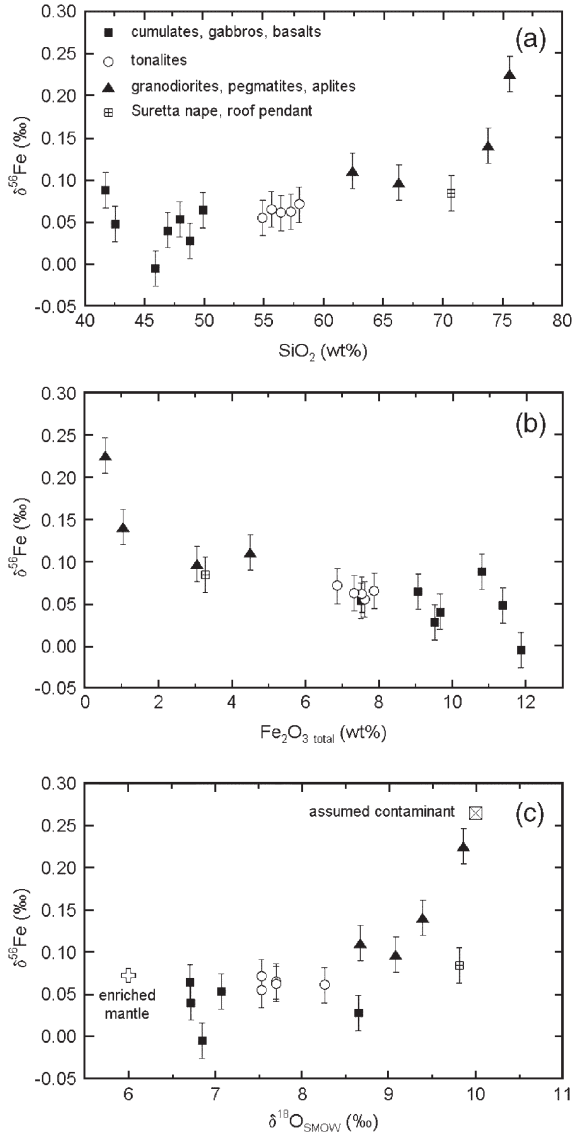

Fig. 4. δ^{56}Fe values versus SiO_2 and total Fe concentrations. (a) Correlation between δ^{56}Fe values and SiO_2 contents of igneous rocks from the calc-alkaline Bergell intrusion, swiss Alps. (b) Inverse correlation between δ^{56}Fe values and total Fe content (given as total Fe_2O_3 in wt.%) of the same sample set. Symbols are the same as in (a). (c) δ^{56}Fe values versus δ^{18}O values of samples from the Bergell igneous rock suite.

4.4.1. Contamination of the Bergell magma with an isotopically heavy assimilant

We can evaluate this possibility with a binary mixing calculation. Considering that the initial Bergell magma had an average basaltic Fe concentration of 10.5 oxide-wt.% (expressed as FeO; [50]) and a δ^{56}Fe value of 0.072‰ (average of basalts given in Table 4), whereas the assimilant had Fe concentrations typical for average lower to middle continental crust and marine pelagic sediments of 6–8.5 oxide-wt.% [51,52]. In this case, isotope mass balance, using the fractions assimilated determined by von Blanckenburg [21] places the assimilant at δ^{56}Fe values of 0.27–0.30‰. With the exception of highly altered oceanic crust [53] or altered extrusive rocks [54], such a heavy (sedimentary) reservoir has so far not been observed (see Fig. 2), although this might be simply due to the fact that pelites have not been mapped for iron isotope compositions in a sufficiently systematic way. Also river suspended loads and modern clastic marine sediments show compositions that are relatively unfractionated compared to average igneous rocks [13,55]. Of all clastic sediments determined by Beard et al. [13] – except the Phanerozoic and Proterozoic shales that are unlikely to exist at lower crustal levels of the Swiss Alps – one single marine sediment has an Fe isotope composition as heavy as that calculated for the Bergell assimilant (i.e. δ^{56}Fe = 0.27–0.30‰; Fig. 2). It needs to be mentioned that the Suretta Nape mainly consists of igneous rocks of the crystalline basement. We therefore consider open-system behaviour involving an assimilant that obtained heavy iron through exogenic processes as unlikely, but not as impossible. Assimilation of granitoid composition rocks containing heavy iron that was previously fractionated by an igneous process (outlined below) is another possibility. In such a case, however, it will be impossible to distinguish whether the fractionation process has taken place during the previous magmatic event forming the assimilant, during the fractional crystallisation that formed the suite under investigation, or as a combination of both events.

4.4.2. Fe isotope fractionation through fractional crystallisation

If fractional crystallisation governs the isotope fractionation during magma differentiation then the process that removes light iron into a liquidus phase has to be identified. Olivine and pyroxenes containing ferrous iron have been predicted from theoretical vibrational frequencies to incorporate the lightest iron when compared to all other silicates [39]. The fractionation factors of these minerals relative to melt are not yet available. However, the fractionation factor $\Delta^{56}Fe_{(pyrrhotite-rhyolitic\ melt)}$ of −0.35‰ at temperatures of 840 to 1000 °C [47] demonstrates that significant Fe isotope fractionation between minerals and melts is possible. This is presumably due to the oxidation state of the melt that contains significant amounts of iron in the ferric state. The change in bond strength associated with the transition to mineral-bound ferrous Fe may entail an

isotope fractionation toward lighter compositions in the crystallising liquidus phases.

The possible effect of fractional crystallisation of a liquidus-phase on the Fe isotope evolution of a melt along a Rayleigh function is illustrated in Fig. 5. Here the fractionation of an initial basaltic melt with a total iron content of 10.5 oxide-wt.% (expressed as total Fe_2O_3) [50] and with the typical basaltic δ^{56}Fe of +0.072‰ has been modelled by removal of an Fe-containing liquidus phase with $\Delta^{56}Fe_{(melt-mineral)}$=0.050‰. The upper solid curve in Fig. 5 shows the instantaneous melt composition which indeed characterises some of the measured rocks. The intermediate stippled curve shows the instantaneous composition of the liquidus phase. The tonalites and the granodiorite plot between these two curves which is expected given that the removal of their liquidus phases from the melt by gravitational settling may not be complete or filter pressing may lead to mixing of melts that are evolved to varying degrees. The lowest curve represents the integrated composition of liquidus phases which would be that of cumulate rocks.

It has to be pointed out that this simplistic model merely serves to illustrate the process by which fractional crystallisation within a single magmatic rock suite might potentially fractionate iron isotopes. In practice, of course, the acting processes are more complex. However, if cumulate minerals preferentially incorporated light iron, then fractional crystallisation may be capable of producing heavy Fe isotope compositions in the order of those observed in Bergell granitoids. It has to be mentioned here, that Beard and Johnson [30] did not find any Fe isotope variations between olivine, amphibole, biotite and magnetite of four andesitic volcanic rocks, but such small isotope differences as predicted from our Rayleigh model with $\Delta^{56}Fe_{(melt-mineral)}$=0.050‰ can hardly be detected at the current reproducibility levels of 0.05–0.10‰.

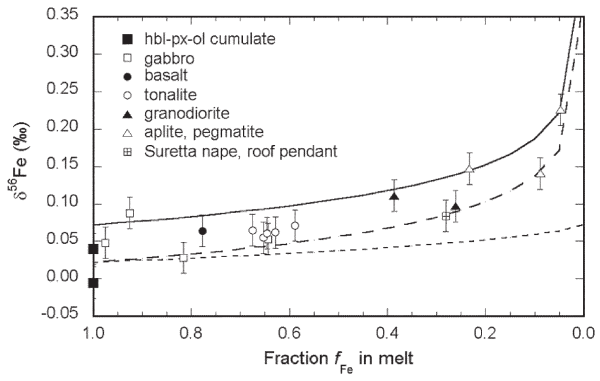

Fig. 5. Comparison of the Fe isotope composition of samples from the Bergell igneous rock suite with a Rayleigh fractionation model that has a starting $\delta^{56}Fe_{(melt)}$ value of +0.072‰ and a constant fractionation factor $\Delta^{56}Fe_{(melt-liquidus\ phase)}$ of +0.050‰. Iron fractions of the Bergell rocks were determined relative to the upper limit Fe concentrations reported for basalts of 10.5 wt.% total Fe_2O_3 [50]. The upper solid curve gives the instantaneous melt composition, the intermediate stippled curve the instantaneous composition of the liquidus-phase, and the lowest stippled curve represents the integrated composition of the liquidus-phase.

5. Conclusions

Despite large variations in δ^{56}Fe values of chondrules, the uniform bulk composition of the different chondrite groups indicates a homogeneous Fe isotope composition for the inner solar system before the onset of chondrule formation. The Fe isotope compositions of HED and martian (SNC) meteorites are indistinguishable to this chondritic baseline. These observations strongly point to the existence of a chondritic uniform reservoir (CHUR) for Fe isotope composition of the inner solar system with a mean δ^{56}Fe value of −0.015 ± 0.020‰ relative to IRMM-014.

The outer liquid core, containing 83% of the Earth's iron, dominates the Fe isotope composition of the bulk Earth. Assuming that Earth's mantle or the bulk silicate Earth had a Fe isotope composition somewhere between −0.13‰ and +0.09‰ in δ^{56}Fe (2 standard deviation limits of our mantle xenoliths), then mass balance places the outer core composition to within ±0.02‰ of the bulk Earth δ^{56}Fe value. These mass balance calculations allow for a possible compositional range of the inner metallic core of as much as δ^{56}Fe=±0.070‰. This range in Fe isotope variations is within the magnitude of predicted equilibrium fractionation between silicate and metal at temperatures prevailing at the core mantle boundary. Within our mass balance parameters the somewhat elevated δ^{56}Fe value of terrestrial basalts of +0.072‰ still fits with a chondritic bulk Earth Fe isotope composition and an inner core approximated by magmatic iron meteorites with δ^{56}Fe=+0.047‰. On the other hand, a kinetic isotope fractionation through partial vaporisation during the giant Moon-forming impact event might also have significantly affected the bulk Earth's iron towards heavier isotope composition [16]. Such impact-related Fe isotope fractionation has recently been proposed for other solar system objects— the CB chondrites ([28]; our Bencubbin chondrule-free matrix).

With the currently available Fe isotope data it is still impossible to prove or disprove Fe isotope fractionation during partial mantle melting. On the one hand it does appear as if the bulk of mantle xenoliths are slightly lighter in Fe isotope compositions than terrestrial basalts (δ^{56}Fe=+0.072‰), thus indicating Fe isotope fractionation by partial mantle melting [1]. On the other hand

mantle xenoliths are highly variable in Fe isotope composition and eucrite/diogenite and SNC meteorites that represent mantle melts of the HED parent body and Mars, respectively, are indistinguishable to the chondritic Fe isotope composition (δ^{56}Fe = −0.015‰).

There is now growing evidence that (at least) high-SiO_2 granitoids are significantly heavier in Fe isotope composition than terrestrial basalts. The process that is responsible for this enrichment in heavy iron, however, is still not clear. Poitrasson and Freydier [20] proposed Fe isotope fractionation during late-stage fluid exsolution from magmas with SiO_2 > 71 wt.%. Our own data indicate that enrichment in heavy iron might already be observed for granitoids with lower SiO_2 contents of 60–70 wt.%. The positive correlation between δ^{56}Fe values and SiO_2 contents of rocks from the Bergell intrusion, Swiss Alps, can be explained by open-system mixing with an isotopically heavy exogenic assimilant (as revealed by AFC modelling using radiogenic Sr and δ^{18}O values [21]). Yet, clastic sediments of such heavy Fe isotope composition have not been reported to date. Alternatively, evolving magmas may be continuously enriched in heavy Fe isotopes through magmatic processes such as fractional crystallisation. However, more detailed studies of uncontaminated crustal rock suites are needed to disclose whether or not crystal fractionation is able to fractionate Fe isotopes.

Acknowledgments

The following persons are thanked for providing samples: B. Hofmann (Museum of Natural History, Bern, Switzerland) for carbonaceous chondrites, B.S. Kamber (Department of Earth Sciences, Laurentian University, Canada) for chondrites and eucrites, and R. Frei (Geological Institute, University of Copenhagen, Denmark) and I.M. Villa (Institute of Geological Sciences, University of Berne, Switzerland) for most of the iron meteorites. The Geoscience Centre of the University of Goettingen, Germany (curator of the collection M. Reich), is greatly thanked for providing peridotite samples ("GZG1275/#") and the Bundesanstalt für Geowissenschaften und Rohstoffe (BGR) in Hannover for XRF major element determinations. A. Pack and J.A. Schuessler are thanked for reading the manuscript and for fruitful discussions. A. Tangen is thanked for her help with sample preparation and Fe separation. F. Poitrasson and an anonymous referee are thanked for their very detailed comments that significantly helped to improve the quality of this work. Associate editor R.W. Carlson is thanked for the editorial handling and helpful comments. We acknowledge financial support by German Research Foundation (DFG) grant SCHO-1071 to R. Schoenberg and H. Behrens.

Appendix A. Supplementary data

Supplementary data associated with this article can be found, in the online version, at doi:10.1016/j.epsl.2006.09.045.

References

[1] S. Weyer, A.D. Anbar, G.P. Brey, C. Munker, K. Mezger, A.B. Woodland, Iron isotope fractionation during planetary differentiation, Earth Planet. Sci. Lett. 240 (2) (2005) 251–264.
[2] A.D. Anbar, J.E. Roe, J. Barling, K.H. Nealson, Nonbiological fractionation of iron isotopes, Science 288 (2000) 126–128.
[3] M. Sharma, M. Polizzotto, A.D. Anbar, Iron isotopes in hot springs along the Juan de Fuca Ridge, Earth Planet. Sci. Lett. 194 (2001) 39–51.
[4] C.J. Johnson, B.L. Beard, N.J. Beukes, C. Klein, J.M. O'Leary, Ancient geochemical cycling in the earth as inferred from Fe isotope studies of banded iron formations from the Transvaal Craton, Contrib. Mineral. Petrol. 144 (2003) 523–547.
[5] S.A. Welch, B.L. Beard, C.M. Johnson, P.S. Braterman, Kinetic and equilibrium Fe isotope fractionation between aqueous Fe(II) and Fe(III), Geochim. Cosmochim. Acta 67 (22) (2003) 4231–4250.
[6] B.L. Beard, C.M. Johnson, Fe isotope variations in modern and ancient Earth and other planetary bodies, in: C.M. Johnson, B.L. Beard, F. Albarède (Eds.), Geochemistry of Non-Traditional Stable Isotopes, Reviews in Mineralogy and Geochemistry, vol. 55, Mineralogical Society of America, Blacksburg, 2004, pp. 319–357.
[7] N. Dauphas, M. van Zuilen, M. Wadhwa, A.M. Davis, B. Marty, P.E. Janney, Clues from Fe isotope variations on the origin of early Archean BIFs from Greenland, Science 306 (5704) (2004) 2077–2080.
[8] A.D. Anbar, Iron stable isotopes: beyond biosignatures, Earth Planet. Sci. Lett. 217 (2004) 223–226.
[9] O.J. Rouxel, A. Bekker, K.J. Edwards, Iron isotope constraints on the Archean and Paleoproterozoic ocean redox state, Science 307 (5712) (2005) 1088–1091.
[10] X.K. Zhu, Y. Guo, R.K. O'Nions, E.D. Young, R.D. Ash, Isotopic homogeneity of iron in the early solar nebula, Nature 412 (6844) (2001) 311–313.
[11] K. Kehm, E.H. Hauri, C.M.O. Alexander, R.W. Carlson, High precision iron isotope measurements of meteoritic material by cold plasma ICP-MS, Geochim. Cosmochim. Acta 67 (2003) 2879–2891.
[12] B.L. Beard, C.M. Johnson, J.L. Skulan, K.H. Nealson, L. Cox, H. Sun, Application of Fe isotopes to tracing the geochemical and biological cycling of Fe, Chem. Geol. 195 (2003) 87–117.
[13] B.L. Beard, C.J. Johnson, K.L. Von Damm, R.L. Poulson, Iron isotope constraints on Fe cycling and mass balance in oxygenated oceans, Geology 31 (2003) 629–632.
[14] J. Völkening, D.A. Papanastassiou, Iron isotope anomalies, The Astrophys. J. 347 (1989) L43–L46.
[15] E. Mullane, S.S. Russell, M. Gounelle, Nebular and asteroidal modification of the iron isotope composition of chondritic components, Earth Planet. Sci. Lett. 239 (3–4) (2005) 203–218.
[16] F. Poitrasson, A.N. Halliday, D.C. Lee, S. Levasseur, N. Teutsch, Iron isotope differences between Earth, Moon, Mars and Vesta as

possible records of contrasted accretion mechanisms, Earth Planet. Sci. Lett. 223 (3–4) (2004) 253–266.
[17] F. Poitrasson, S. Levasseur, N. Teutsch, Significance of iron isotope mineral fractionation in pallasites and iron meteorites for the core–mantle differentiation of terrestrial planets, Earth Planet. Sci. Lett. 234 (1–2) (2005) 151–164.
[18] X.K. Zhu, Y. Guo, R.J.P. Williams, R.K. O'Nions, A. Matthews, N.S. Belshaw, G.W. Canters, E.C. de Waal, U. Weser, B.K. Burgess, B. Salvato, Mass fractionation processes of transition metal isotopes, Earth Planet. Sci. Lett. 200 (1–2) (2002) 47–62.
[19] H.M. Williams, A.H. Peslier, C. McCammon, A.N. Halliday, S. Levasseur, N. Teutsch, J.-P. Burg, Systematic iron isotope variations in mantle rocks and minerals: the effects of partial melting and oxygen fugacity, Earth Planet. Sci. Lett. 235 (1–2) (2005) 435–452.
[20] F. Poitrasson, R. Freydier, Heavy iron isotope composition of granites determined by high resolution MC-ICP-MS, Chem. Geol. 222 (1–2) (2005) 132–147.
[21] F. von Blanckenburg, G. Fruhgreen, K. Diethelm, P. Stille, Nd-isotopic, Sr-isotopic, O-isotopic and chemical evidence for a 2-stage contamination history of mantle magma in the Central-Alpine Bergell intrusion, Contrib. Mineral. Petrol. 110 (1) (1992) 33–45.
[22] R. Schoenberg, F. von Blanckenburg, An assessment of the accuracy of stable Fe isotope ratio measurements on samples with organic and inorganic matrices by high-resolution multicollector ICP-MS, Int. J. Mass Spectrom. 242 (2–3) (2005) 257–272.
[23] P.D.P. Taylor, R. Maeck, P. DeBievre, Determination of the absolute isotopic composition and atomic-weight of a reference sample of natural iron, Int. J. Mass Spectrom. Ion Process. 121 (1992) 111–115.
[24] S. Weyer, J. Schwieters, High precision Fe isotope measurements with high mass resolution MC-ICPMS, Int. J. Mass Spectrom. 226 (2003) 355–368.
[25] G.L. Arnold, S. Weyer, A.D. Anbar, Fe isotope variations in natural materials measured using high mass resolution multiple collector ICPMS, Anal. Chem. 76 (2) (2004) 322–327.
[26] N. Dauphas, P.E. Janney, R.A. Mendybaev, M. Wadhwa, F.M. Richter, A.M. Davis, M. van Zuilen, R. Hines, C.N. Foley, Chromatographic separation and multicollection-ICPMS analysis of iron. Investigating mass-dependent and-independent isotope effects, Anal. Chem. 76 (19) (2004) 5855–5863.
[27] K.R. Ludwig, ISOPLOT— A Plotting and Regression Program for Radiogenic Isotope Data, USGS open file report 91–445 (1994).
[28] J. Zipfel, S. Weyer, Impact or solar nebula origin of CB chondrites? Evidence from Fe isotopes, Lunar and Planetary Science Conference, Houston, vol. XXXVII, 2006, p. 1902.
[29] I. Horn, F. von Blanckenburg, R. Schoenberg, G. Steinhoefel, G. Markl, In situ iron isotope ratio determination using UV-femtosecond laser ablation with application to hydrothermal ore formation processes, Geochim. Cosmochim. Acta 70 (14) (2006) 3677–3688.
[30] B.L. Beard, C.M. Johnson, Inter-mineral Fe isotope variations in mantle-derived rocks and implications for the Fe geochemical cycle, Geochim. Cosmochim. Acta 68 (22) (2004) 4727–4743.
[31] H.M. Williams, C.A. McCammon, A.H. Peslier, A.N. Halliday, N. Teutsch, S. Levasseur, J.P. Burg, Iron isotope fractionation and the oxygen fugacity of the mantle, Science 304 (5677) (2004) 1656–1659.
[32] S. Weyer, C. Munker, G.P. Brey, A.B. Woodland, K. Mezger, A.D. Anbar, Iron Isotope Fractionation During Planetary Differentiation Processes, European Geosciences Union, Vienna, 2005.
[33] B.A. Cohen, R.H. Hewins, C.M.O. Alexander, The formation of chondrules by open-system melting of nebular condensates, Geochim. Cosmochim. Acta 68 (7) (2004) 1661–1675.
[34] B.A. Cohen, S. Levasseur, B. Zanda, R.H. Hewins, A.N. Halliday, Kinetic isotope effect during reduction of iron from a silicate melt, Geochim. Cosmochim. Acta 70 (12) (2006) 3139–3148.
[35] J.W. Morgan, E. Anders, Chemical-Composition of Earth, Venus, and Mercury, Proc. Natl. Acad. Sci. U. S. A.,—Phys. Sci. 77 (12) (1980) 6973–6977.
[36] S.R. Taylor, S.M. McLennan, The composition and evolution of the continental-crust— rare-Earth element evidence from sedimentary-rocks, Philos. Trans. - Royal Soc., Math. Phys. Eng. Sci. 301 (1461) (1981) 381–399.
[37] C.J. Allegre, J.P. Poirier, E. Humler, A.W. Hofmann, The chemical-composition of the Earth, Earth Planet. Sci. Lett. 134 (3–4) (1995) 515–526.
[38] C. Yoder, Astrometric and Geodetic Properties of Earth and the Solar System, in: T.J. Ahrens (Ed.), Global Earth Physics: A Handbook of Physical Constants, American Geophysical Union, Washington, 1995, p. 376.
[39] V.B. Polyakov, S.D. Mineev, The use of Mössbauer spectroscopy in stable isotope geochemistry, Geochim. Cosmochim. Acta 64 (2000) 849–865.
[40] J. Li, C.B. Agee, Geochemistry of mantle–core differentiation at high pressure, Nature 381 (6584) (1996) 686–689.
[41] K. Righter, M.J. Drake, G. Yaxley, Prediction of siderophile element metal–silicate partition coefficients to 20 GPa and 2800 degrees C: the effects of pressure, temperature, oxygen fugacity, and silicate and metallic melt compositions, Phys. Earth Planet. Inter. 100 (1–4) (1997) 115–134.
[42] C.K. Gessmann, D.C. Rubie, The origin of the depletions of V, Cr and Mn in the mantles of the Earth and Moon, Earth Planet. Sci. Lett. 184 (1) (2000) 95–107.
[43] N.L. Chabot, M.J. Drake, Crystallization of magmatic iron meteorites and liquid immiscibility in the iron–phosphorus–sulfur system, Meteorit. Planet. Sci. 34 (1999) A22–A23.
[44] N.L. Chabot, M.J. Drake, Crystallization of magmatic iron meteorites: the effects of phosphorus and liquid immiscibility, Meteorit. Planet. Sci. 35 (4) (2000) 807–816.
[45] J.P. Poirier, Light-elements in the Earths outer core— a critical-review, Phys. Earth Planet. Inter. 85 (3–4) (1994) 319–337.
[46] B.J. Wood, A.N. Halliday, Cooling of the Earth and core formation after the giant impact, Nature 437 (7063) (2005) 1345–1348.
[47] J.A. Schuessler, R. Schoenberg, H. Behrens, F. von Blanckenburg, The experimental calibration of the iron isotope fractionation factor between pyrrhotite and peralkaline rhyolitic melt, Geochim. Cosmochim. Acta (in press), doi:10.1016/j.gca.2006.09.012.
[48] K. Righter, M.J. Drake, Core formation in Earth's Moon, Mars, and Vesta, Icarus 124 (2) (1996) 513–529.
[49] N. Dauphas, O. Rouxel, Mass spectrometry and natural variations of iron isotopes, Mass Spectrom. Rev. 25 (4) (2006) 515–550.
[50] K.C. Condie, Chemical-composition and evolution of the upper continental-crust— contrasting results from surface samples and shales, Chem. Geol. 104 (1–4) (1993) 1–37.
[51] R.L. Rudnick, D.M. Fountain, Nature and composition of the continental-crust— a lower crustal perspective, Rev. Geophys. 33 (3) (1995) 267–309.
[52] T. Plank, C.H. Langmuir, The chemical composition of subducting sediment and its consequences for the crust and mantle, Chem. Geol. 145 (3–4) (1998) 325–394.

[53] O. Rouxel, N. Dobbek, J. Ludden, Y. Fouquet, Iron isotope fractionation during oceanic crust alteration, Chem. Geol. 202 (1–2) (2003) 155–182.

[54] K.E. Yamaguchi, C.M. Johnson, B.L. Beard, H. Ohmoto, Biogeochemical cycling of iron in the Archean-Paleoproterozoic Earth: constraints from iron isotope variations in sedimentary rocks from the Kaapvaal and Pilbara Cratons, Chem. Geol. 218 (1–2) (2005) 135–169.

[55] C.M. Johnson, B.L. Beard, F. Albarède, Geochemistry of Non-Traditional Stable Isotopes, in: J.J. Rosso (Ed.), Reviews in Mineralogy and Geochemistry, vol. 55, Mineralogical Society of America, Blacksburg, 2004.

[56] M. Staubwasser, F. von Blanckenburg, R. Schoenberg, Iron isotopes in the early marine diagenetic iron cycle, Geology 34 (8) (2006) 629–632.